Molecular Catalysis 501 (2021) 111363

Contents lists available at ScienceDirect

Molecular Catalysis

journal homepage: www.journals.elsevier.com/molecular-catalysis

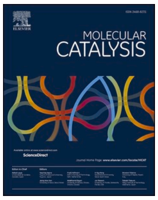

Highly efficient and selective one-pot tandem imine synthesis via amine-alcohol cross-coupling reaction catalysed by chromium-based MIL-101 supported Au nanoparticles

Ilkay Gumus [a,b,*,1], Adem Ruzgar [c], Yasar Karatas [c], Mehmet Gülcan [c,1,*]

[a] *Advanced Technology Applied and Research Center, Mersin University, Mersin, 33343, Turkey*
[b] *Department of Basic Sciences, Faculty of Maritime, Mersin University, Mersin, 33343, Turkey*
[c] *Department of Chemistry, Van Yüzüncü Yıl University, Van, 65080, Turkey*

ARTICLE INFO

Keywords:
Au NPs
Catalyst
Cross-coupling reaction
Imine synthesis
MIL-101

ABSTRACT

One-pot tandem synthesis of imines from alcohols and amines is regarded as an effective, economic and green approach under mild conditions. In this work, Au nanoparticles (NPs) dispersed on MIL-101 (Au/MIL-101) were demonstrated as highly active and selective bifunctional heterogeneous catalyst for production of various imine derivatives with excellent yields, via amine-alcohol cross-coupling reaction at 343 K in an open flask under an Ar atmosphere. Various physicochemical techniques, including inductively coupled plasma optical emission spectroscopy (ICP-OES), powder X-ray diffraction (P-XRD), X-ray photoelectron spectroscopy (XPS) transmission electron microscopy (TEM) and N_2 adsorption-desorption, were used to characterize of the Au/MIL-101 catalyst. The obtained bifunctional catalyst is highly active and selective towards one-pot imine formation and exhibited the highest TOF (30.15-51.47 h^{-1}) among all the ever-reported MOF-supported Au catalysts. The reaction mechanism of the imine formation from alcohol and amine over Au/MIL-101 catalyst was proposed. Mechanism experiment results demonstrate that Au NPs highly effective in activating oxidation of benzyl alcohol to benzaldehyde while the Lewis acid sites on MIL-101 catalyzed the second condensation step without interfering with the oxidation step. As a result, the excellent catalytic performance of Au/MIL-101 can be ascribed to the synergistic effect between Au NPs with Lewis acid sites in MIL-101.

1. Introduction

Tandem reactions have recently attracted increasing attention due to sustainable green processes that show the concepts of efficiency and atomic economy. In these reactions two or more successive individual reactions occur realized in a one-pot system without purifying and separating the byproducts [1–6]. In tandem reactions, main aim is to obtain high selectivity and activity towards a single product and these reactions often require the oxidation or reduction steps to be combined with others such as Knoevenagel condensation [1,2,7]. To achieve this combination, tandem reactions are supported by two catalysts or a bifunctional catalyst having two or more types of active sites [1].

MOFs are particularly appropriate materials for tandem reactions because they can have two or more different active centres such as metal nodes, guest species in the pores and functional organic linkers [1,5,6,8–16]. For example, the dispersed/encapsulated Au NPs on/inside MOFs can have oxidation or reduction activity, while the metal nodes or the functional organic linkers of support can have the second type of active sites [17,18]. On the other hand, compared to other porous materials such as mesoporous silica and zeolites, the properties of MOFs are logically “designable” to examine the effect of the chemical environment on the dispersed/encapsulated metal NPs. Because the metal nodes and the functional organic linkers of MOFs can be fine-tuned either by utilizing different groups or by the post-synthetic modification of pre-synthesized MOFs [19–22]. The introduction of various groups such as $-NH_2$, $-SO_3H$, LiOEt, LiO^tBu, AcO to isoreticular MOFs can significantly affect activity, stability, and mechanical properties of the MOFs [23–27].

Recently, monometallic and bimetallic NPs encapsulated/dispersed on/inside MOFs that catalyze various tandem reactions have been

---

* Corresponding authors.
E-mail addresses: gumus.ilkay84@gmail.com (I. Gumus), mehmetgulcan65@gmail.com (M. Gülcan).

[1] Website: https://avesis.yyu.edu.tr/mehmetgulcan.

https://doi.org/10.1016/j.mcat.2020.111363
Received 7 September 2020; Received in revised form 26 November 2020; Accepted 16 December 2020

reported [28–31]. Chen et. al. reported monometallic and bimetallic NPs@MOF (Pd@MIL-101 and PdAg@MIL-101) catalysts with tiny metal NPs inside MOFs for the one-pot tandem synthesis of secondary arylamine [32]. The results showed that MIL-101 provides Lewis acid sites (chromium centres) and Pd offers hydrogenation activity while Ag greatly improves selectivity toward the corresponding secondary amine. Li et. al. reported bimetallic Pt–Ni frames into porous MOF-74 for the one-pot tandem reductive imination of nitroarenes with carbonyl compounds [33]. Qi et al. reported bifunctional Au/MIL-53(NH_2) catalyst for synthesis of 2-benzylidenemalononitrile and its derivatives *via* one-pot alcohol oxidation/Knoevenagel condensation reactions. The results display that Au NPs only promote the first oxidation step, and the amino groups catalyze the second condensation step without interfering with the first step [34].

Over the last decades, remarkable efforts have been devoted to the direct synthesis of various imines, in particular via one-pot tandem procedures because they can be further transformed into various biologically and pharmaceutically active compounds such as β-lactams, aziridines and benzoxazole benzimidazole [35,36]. According to the widely accepted reaction mechanism of one-pot imines formation from alcohols and amines, during cross-coupling reactions of alcohol-amine, alcohol is first oxidized to corresponding aldehyde (under aerobic condition) which is then reacted with unreacted amine to form the secondary imine (under aerobic condition) [31,37,38]. This process is very challenging because if both alcohols and amines are in the same reaction mixture, there are many possible side reactions and many byproducts such as amides [39], acids [40], diazo compounds [41] and esters [42] can be obtained depending on the nature of the catalyst used and the reaction conditions selected (Scheme 1). Thereby, the design of an effective heterogeneous catalyst to prevent the unnecessary side reactions requires a combination of a metallic functional moiety for alcohol oxidation step and an acidic functional part for condensation step.

In this work, we have developed a simple and efficient method for the selective synthesis of imines from alcohols and amines *via* one-pot prosess using a new readily recoverable bifunctional catalyst that combines the catalytic activity of Au NPs with the active centers of MIL-101. The Au/MIL-101 catalyst showed excellent activity, selectivity, stability and substrate scope towards one-pot imine formation, offering the highest TOFs among ever reported MOF-supported Au catalysts in the literature. We also examined the effect of various reaction parameters (such as temperature, base, oxygen) as well as Au NPs and MIL-101 solid support structure on catalytic activity.

2. Experimental

2.1. Materials and reagents

Gold (III) chloride trihydrate ($HAuCl_4 \cdot 3H_2O$), chromium trinitrate nonahydrate ($Cr(NO_3)_3 \cdot 9H_2O$), terephthalic acid ($C_8H_6O_4$), methanol (CH_3OH), acetone (CH_3COCH_3), sodium borohydride ($NaBH_4$), benzyl alcohol and amine derivatives were supplied from common commercial sources such as Merck, TCI and Sigma-Aldrich®. Toluene dried by using standard procedure. Water was purified by reversed osmosis with ion exchange and used as a solvent for the preparation of reagents solution and dilution (Human RO 180 brand water purifier). In addition, the glass and other materials needed in all studies were used by washing with chromic acid cleaning solution, water and acetone and drying.

2.2. Instrumentation

The exact Au loading was measured by the inductively coupled plasma optical emission spectroscopy (ICP-OES) technique on an Perkin Elmer DRC II model. The powder X-ray diffraction (P-XRD) analyses were carried out on Rigaku Ultima-IV by using Cu-Kα radiation (wavelength 1.54 Å, 40 kV, 55 mA). X-ray photoelectron spectroscopy (XPS) analysis was performed under ultra-high vacuum on a Physical Electronics 5800 spectrometer equipped with a hemispherical analyzer and using monochromatic Al- Kα radiation (1486.6 eV, the X-ray tube working at 15 kV and 350 W, and pass energy of 23.5 eV). The binding energy shift due to the surface charging was adjusted using a reference to the C 1s line at 284.5 eV. The surface morphology and microstructure of Au/MIL-101 catalyst was determined by using conventional transmission electron microscope (TEM, JEOL JEM-200CX, 120 kV), equipped with energy dispersed X-ray detector (EDX) and high resolution transmission electron microscope (HR-TEM, JEOL JEM-2010F, 200 kV). Fourier transform infrared (FT-IR) spectra were performed on a Bio-Rad-Win-IR spectrophotometer instrument in the range of between 4000 and 400 cm^{-1}. The NMR spectra were recorded in $CDCl_3$ solvent on Bruker Avance III 400 MHz NaNoBay FT-NMR spectrophotometer using tetramethylsilane as an internal standard. Gas chromatography (GC-FID) analyses were performed were performed on Shimadzu GC-2010 Plus. The N_2 adsorption-desorption experiment was carried out at 77 K using a Micrometrics Surface Area and Porosity instrument (MicroActive for TriStar II Plus 2.00).

2.3. Synthesis and purification of MIL-101(Cr) and MIL-101(Cr) stabilized gold NPs (Au/MIL-101)

MIL-101 host matrix is prepared by hydrothermal synthesis method, which is frequently used in the literature reports [43–45], and purified

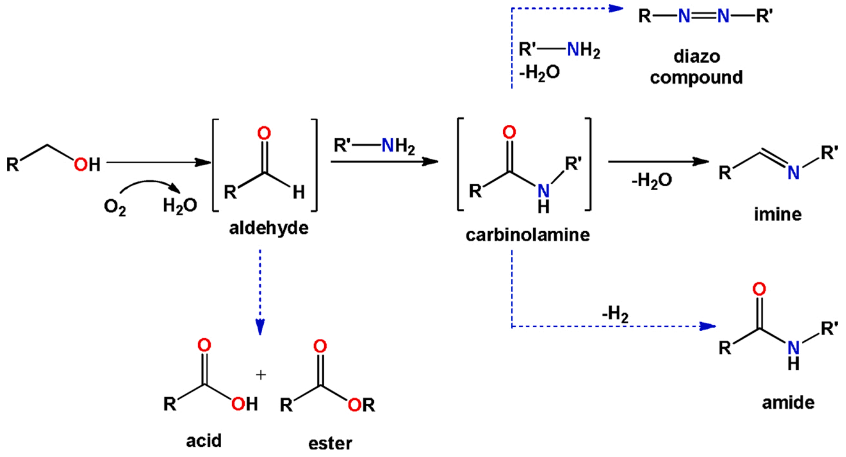

Scheme 1. Possible pathways for the imine formation from alcohol and amine.

from impurities. Au NPs stabilized with MIL-101 support (Au/MIL-101) were synthesized with a simple impregnation-reduction approach [45–47]. Detailed synthesis protocols for the synthesis of both MIL-101 host matrix and Au/MIL-101 catalyst are provided as Supplementary Material.

2.4. *General experimental procedure for one-pot tandem synthesis of imines*

Typically, benzyl alcohol (0.625 mmol), amine (0.625 mmol), KO^{t}Bu (0.20 mmol), 5 ml of toluene and Au/MIL-101 (20 mg) was added successively. Then, the reaction mixture was stirred (900 rpm) at 343 K for 8 h in open system (to allow air to pass into the reaction medium) under an Ar atm. After cooling, ethyl acetate was added to dilute the reaction mixture and the catalyst was centrifuged from the solution. Then, solution filtered through a short pad of SiO_2 column. The filtrate was analysed by GC and NMR techniques (**Figs. S1-S20**).

2.5. *Reusability experiments*

The reaction between 4-chlorobenzylamine and benzyl alcohol was monitored as a model reaction for reusability tests. After the completion of the first reaction, the catalyst was separated by centrifugation (6000 rpm for 15 min), washed with ethanol, ethyl acetate and deionized water, dried at 70 °C for 12 h under vacuum, and was used for the next runs under the same reaction conditions.

2.6. *Leaching test*

The Au/MIL-101 catalyst was separated from the reaction mixture after 3 h. The filtrate transferred to a new vial and the reaction was carried out under the same conditions for an additional 5 h.

3. Result and discussion

3.1. *Characterization of MIL-101(Cr) and Au/MIL-101 catalyst*

The detailed morphology of Au/MIL-101 catalyst was investigated *via* TEM, TEM-EDX and HR-TEM. Fig. 1 shows the low resolution TEM images of Au/MIL-101 catalyst in different scale. As depicted in Fig. 1, the Au NPs are well dispersed on MIL-101 host matrix surface and large-sized gold agglomerates were not formed on the MIL-101 surface. Fig. 2 (a) and (b) demonstrates the TEM image in 50 nm scale and associated particle size histogram of Au/MIL-101 catalyst. According to the particle size analysis using the NIH image program [48], the mean particle size of the Au (0) NPs in the Au/MIL-101 catalyst was determined to be 1.94 ± 0.16 nm. The corresponding EDX analysis of Au/MIL-101 catalyst further indicates the existence of Au, Cr, C, and O elements (Fig. 2 (c)). The HR-TEM image (Fig. 2 (d)) shows the lattice fringes of Au/MIL-101 catalyst with D-spacing of 0.237 nm, confirming the formation of Au (111) planes [49,50].

XPS measurements were performed to reveal the elemental compositions and electronic structure of Au/MIL-101 catalyst. The survey XPS spectrum for Au/MIL-101 catalyst shows the co-existence of Au, Cr, C, and O (Fig. 3 (a)). As shown in Fig. 3 (b), the binding energies for Au $4f_{7/2}$ and Au $4f_{5/2}$ at 82.5 and 86.1 eV are clearly observed in Au 4f XPS spectrum, which could be assigned to states of Au (0) [51,52] In addition, the binding energies for Au $4f_{7/2}$ and Au $4f_{5/2}$ at 83.7 and 87.0 eV are corresponded to Au (III), which could be explained by the surface oxidation of Au during the sample preparation process for XPS test and/or unreduced species of Au [51,53].

The crystal structures of MIL-101 and Au/MIL-101 samples were characterized by P-XRD (Fig. 4). The characteristic diffraction peaks of MIL-101 can be apparently observed in Fig. 4, indicating the successful formation of MIL-101 crystals [43–45]. The characteristic diffraction peaks of MIL-101 crystal are still retained after loading of metal NPs, suggesting the crystalline structure of MIL-101 is stable during the catalyst preparation. Additionally, the wide-angle XRD pattern of Au/MIL-101 catalyst shows a broad and weak diffraction peaks at 2θ = 38.34, 44.76, 65.14 and 77.96°, assigned to (111), (200), (220) and (311) planes of a face-centered cubic (*fcc*) crystal structure of gold ((Joint Committee on Powder Diffraction Standards-JCPDS no. 04-0784, USA) [54,55].

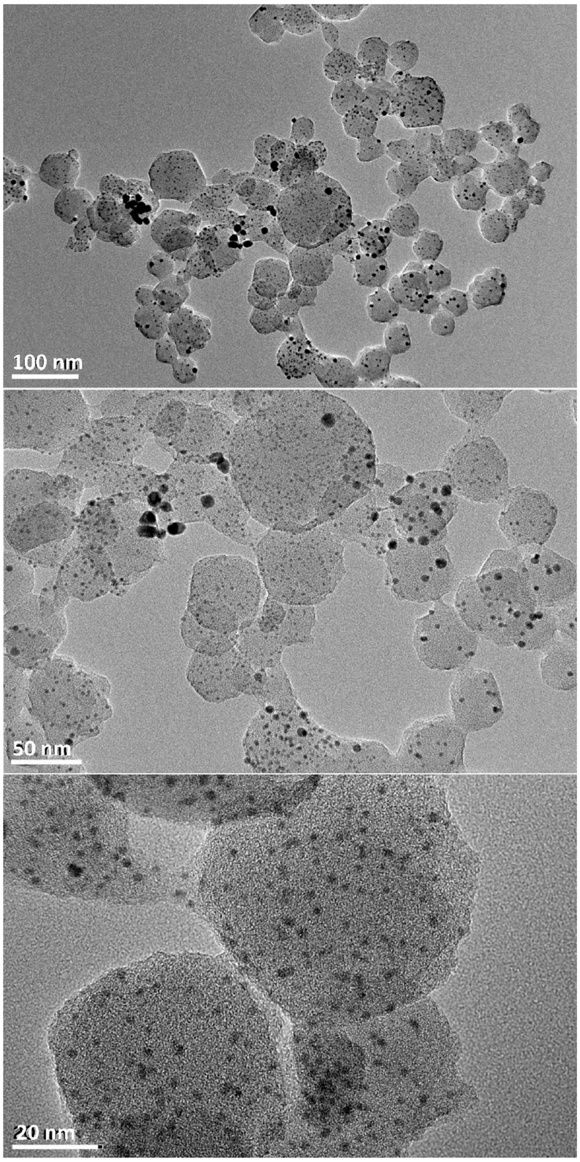

Fig. 1. Low resolution TEM images in different scale of Au/MIL-101 catalyst.

Characteristic IR bands of MIL-101 and Au/MIL-101 catalyst are compared in Fig. 5. When the spectrum is examined, two bands resulting from stretching and bending are seen at 3433 and 1625 cm^{-1}. The signals seen in these band intervals are caused by the adsorbed water on the surface of MIL-101. The band observed at 1402 cm^{-1} is caused by symmetrical (O—C—O) vibrations in the structure of terephthalic acid. The presence of this band in the IR spectrum confirms the presence of terephthalic acid in the structure of MIL-101. The signals observed between 600 cm^{-1} and 1600 cm^{-1} result from the benzene ring in the structure. The bond structure in the benzene ring (C=C) causes tension vibrations at 1508 cm^{-1}. Other signals from the benzene ring are seen in 1107, 1020, 749 and 663 cm^{-1} [56–61]. When comparing IR spectrum of Au/MIL-101 catalyst with MIL-101 spectrum; In both spectra, the peaks appear in the same band regions. These results are considered to

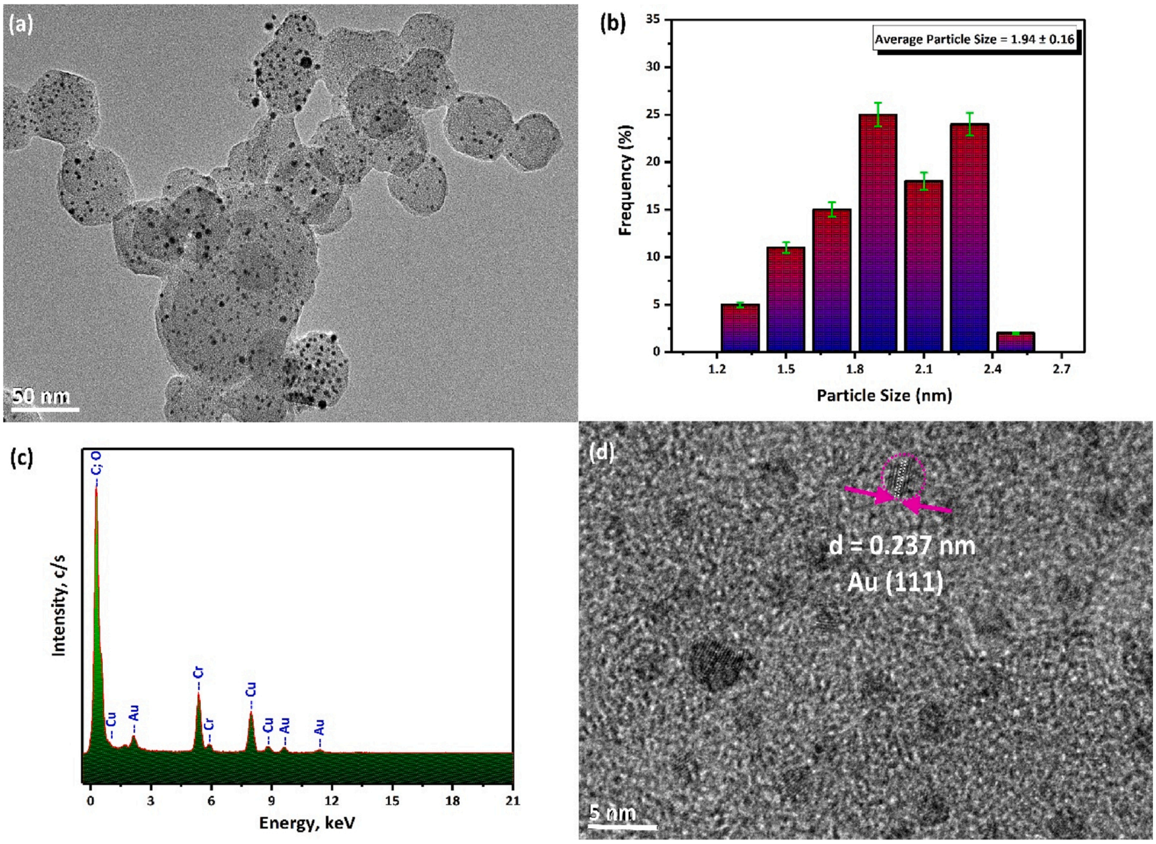

Fig. 2. (a) TEM image in 50 nm scale, (b) associated particle size histogram, (c) related EDX spectrum and (d) HR-TEM image in 5 nm scale of Au/MIL-101 catalyst.

be evidence of no degradation in the structure of the MIL-101 during the preparation of the Au/MIL-101 catalyst [61].

N_2 adsorption-desorption isotherms of MIL-101 and Au/MIL-101 are given in **Figs. S21** and **S22**. MIL-101 and Au/MIL-101 show type I shape nitrogen adsorption-desorption isotherms, which is a characteristic for microporous materials [62]. The micropore volumes and surface areas for MIL-101 and Au/MIL-101 were established by the *t*-plot method [63]. On passing from MIL-101 to Au/MIL-101, both the micropore volume (from 1.26 cm^3/g to 1.17 cm^3/g) and BET surface area (from 2399.62 m^2/g to 2104.79 m^2/g) are prominently reduced. The considerable decrease observed in the micropore volume and surface area for Au/MIL-101 can be attributed to the encapsulation of gold nanoparticles in MIL-101 or their deposition on the cage windows of MIL-101. Furthermore, hysteresis loop was not observed in the N_2 adsorption-desorption isotherm of Au/MIL-101 and pore size distribution was found to be changed in the same manner that of MIL-101 framework which reveals that the synthesis protocol followed in the preparation of Au/MIL-101 did not create any mesopores in MIL-101 framework [44,45].

3.2. *The catalytic efficiency of Au/MIL-101 catalyst in the imine production from the coupling of alcohols and amines*

After the successful preparation of Au/MIL-101 catalysts with different Au content, their catalytic performances were evaluated for the one-pot tandem imine synthesis *via* amine-alcohol cross-coupling reaction. The large surface area, structure stability, rich Lewis acid active region of MIL-101 caused us to choose it as the host matrix for Au NPs [2,12,14]. Because the porous cage structure and large surface area can be used to stabilize the ultra-small Au NPs (*ca.* 1.92 nm).

Reactivity of the catalysts in one-pot tandem reaction was studied using benzyl alcohol and 4-chlorobenzylamine as model substrates. According to the widely accepted reaction process for one-pot formation of imines from alcohols and amines, alcohol is first oxidized to corresponding aldehyde (oxidation step under aerobic conditions and catalysed step) which is then reacted with amine to form the secondary imine (condensation step under anerobic conditions and sometimes uncatalysed step) [31,37,38,56–58,61]. Thereby, design and production of active centers for selectively oxidize alcohols to the related aldehydes remains no doubt crucial for obtaining high yield of imines. The selective oxidation of benzyl alcohol to benzaldehyde is the key step for this tandem reaction, and in this step, by-products such as benzoic acid and benzyl benzoate may occur depending on the nature of the catalyst used and the reaction conditions selected. To achieve the maximum conversion and selectivity in this step, we first optimized the conversion of benzyl alcohol (Step 1), which is the rate-determining step for this one-pot reaction. Meanwhile, the control experiment was carried out without catalyst and considerable bezaldehyde yield was not observed (Table 1, entry 1).

Initially, for comparison, the selective oxidation of benzyl alcohol to benzaldehyde was evaluated using the Au/MIL-101 catalysts with different Au content (0.5, 1.0, 2.0, 3.0 and 4.0 wt % Au) by keeping the other reaction parameters constant (*i.e.* 0.625 mmol of benzyl alcohol, 0.20 mmol of KO^tBu, 20 mg of catalyst, 343 K, air atmosphere). As the Au content of catalyst is increased up to wt 3%, the yield of benzaldehyde was gradually increased. Interestingly, when the amount of Au content increases to 4%-Au/MIL-101, the yield of the related aldehyde also decreased to 76 %. This decrease in activity might be explained by the many Au NPs aggregated in the surface of the MIL-101 support [31]. Thereby, 3%-Au/MIL-101 is an optimum catalyst with 99 % conversion of benzyl alcohol and with 99 % selectivity of benzaldehyde (Table 1, entries 2–6).

To understand the effect of oxygen on reactivity, the same reaction was also investigated in the Ar atmosphere (sealed system) under tested conditions. As shown in Table 1, the yield of benzaldehyde product was trace amount (Table 1, entry 7). Therefore, it can be said that the

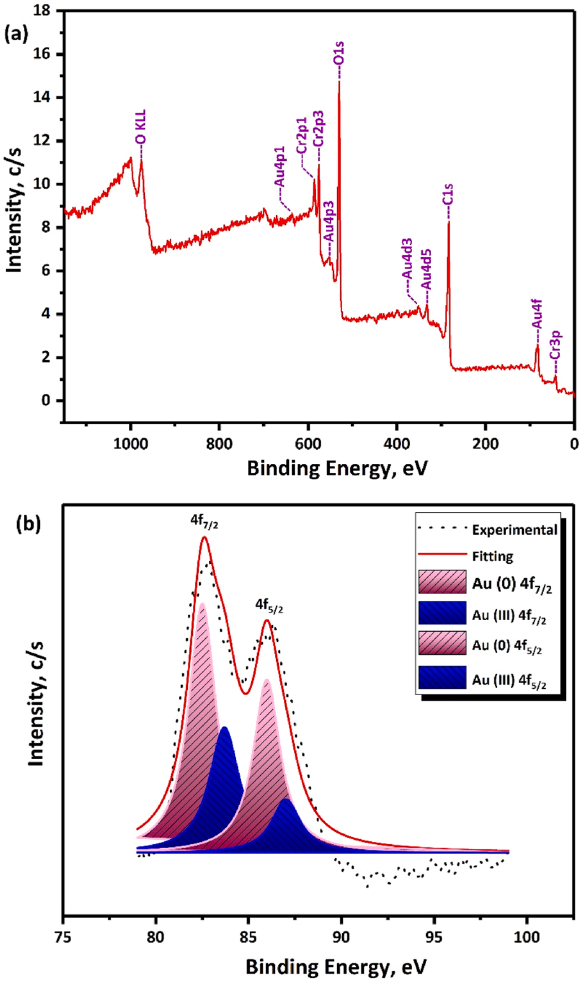

Fig. 3. (a) Survey and (b) Au 4f core level high resolution XPS spectra of Au/MIL-101 catalyst.

presence of oxygen is important for this reaction. Similarly, the reaction did not proceed in the absence of the base (Table 1, entry 8). Thus, we searched the influence of various bases such as Na_3PO_4, Cs_2CO_3, K_2CO_3, and KO^{t}Bu with different dissociation constants (pK_a) values and the results are summarized in Table 1 (entries 9–11). As can be seen from the Table 1, the benzyl alcohol conversion after 7 h of reaction follows almost the same order as the pK_a: KO^{t}Bu $>$ Na_3PO_4 $>$ K_2CO_3 $\approx$ Cs_2CO_3, this most probably associated to the concentration of benzyloxide species that are involved in the first step of the reaction [64].

It is generally accepted that the role of the base is to form an alcoholate that will bind to the unsaturated Au atoms [2,59]. Although elaborations about this subject are still not known, the key point in the oxidation step is proposed to be the transfer of a α-H from the alcoholate to Au. To confirm this and understand the effect of Au NPs in oxidation step, we screened the oxidation of benzyl alcohol with bare MIL-101 as catalyst without Au NPs, and only 5% of benzaldehyde was obtained (Table 1, entry 12). As a result, it can be said that Au NPs are crucial for the catalytic reactivity in the selective oxidation reaction of benzyl alcohol and the oxidation reaction proceeds through the Au atoms in the presence of a base.

Subsequently, with the optimal 3.0 %-Au/MIL-101 as catalyst and optimal KO^{t}Bu as base, various solvents were also examined for this transformation. Because, the catalytic activity is considerably affected by the solvent. Every solvent has specific properties like acid–base behavior, chemical constitution, boiling point, solute–solvent interaction, thermal stability, oxygen's solubility *etc.* which are important to a chemical process. Especially, thermal conductivity of solvent influences catalyst NPs activation and eventually conversion. Solvent with high thermal conductivity leads increase in the particle thermal conduction which results in the activation of catalyst and hereby needs lower activation energy for conversion [65]. In the oxidation reactions, activity may also be affected by the solubility of oxygen in the solvent. The oxidation of benzyl alcohol to benzaldehyde increases with increased oxygen demand, so the solvent that can dissolve more oxygen will lead to high conversion. The highest conversion was achieved with nonpolar

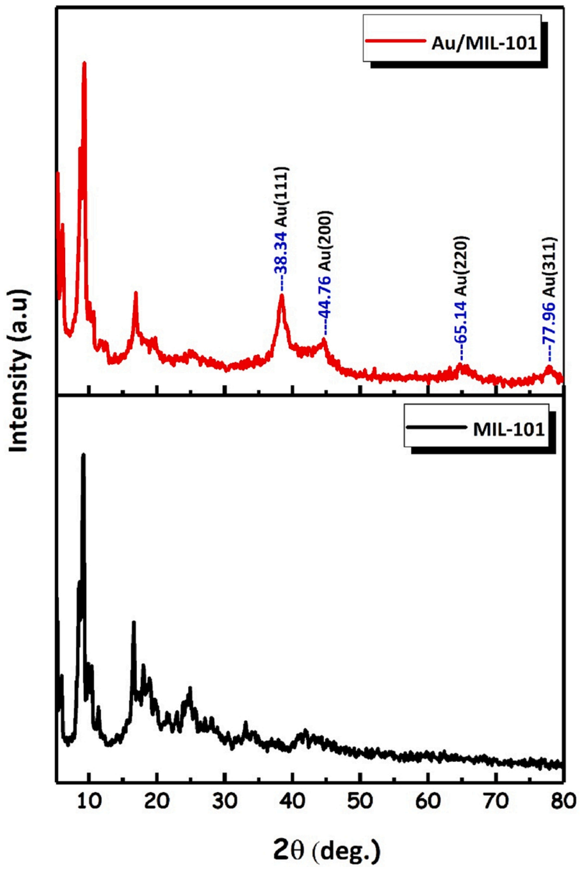

Fig. 4. Wide angle P-XRD patterns of MIL-101 and Au/MIL-101 catalyst (5.0 wt % Au) in the range of 2θ = 5-80°.

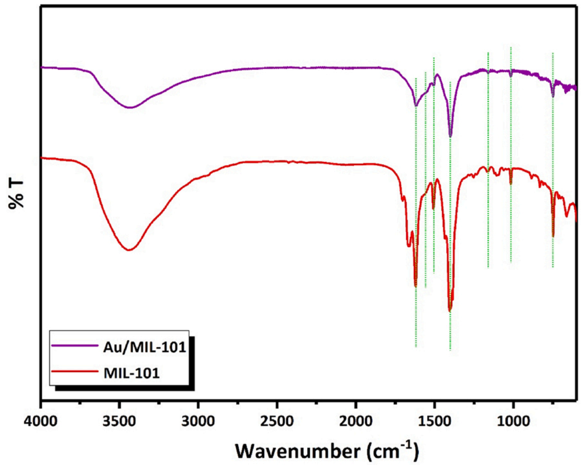

Fig. 5. FT-IR spectra of MIL-101 and Au/MIL-101 catalyst in the range of 4000-400 cm^{-1}.

Table 1
Optimization of benzyl alcohol oxidation with Au/MIL-101[a].

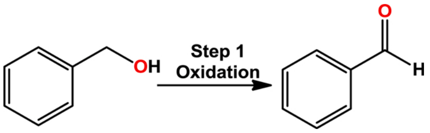

Entry	Catalyst	Base	Time (h)	Temp. (K)	Conditions	Conv. (%)
1	None	KO^tBu	24	343	Air	trace
2	0.5%-Au/MIL-101	KO^tBu	7	343	Air	29
3	1.0%-Au/MIL-101	KO^tBu	7	343	Air	51
4	2.0%-Au/MIL-101	KO^tBu	7	343	Air	68
5	3.0 %-Au/MIL-101	KO^tBu	7	343	Air	99
6	4.0%-Au/MIL-101	KO^tBu	7	343	Air	76
7	3.0 %-Au/MIL-101	KO^tBu	24	343	Sealed flask/Ar	trace
8	3.0 %-Au/MIL-101	None	24	343	Air	trace
9	3.0 %-Au/MIL-101	Cs_2CO_3	7	343	Air	32
10	3.0 %-Au/MIL-101	K_2CO_3	7	343	Air	44
11	3.0 %-Au/MIL-101	Na_3PO_4	7	343	Air	62
12	MIL-101	KO^tBu	24	343	Air	5
13	3.0 %-Au/MIL-101	1,4-dioxane	20	343	Air	26
14	3.0 %-Au/MIL-101	DMSO	20	343	Air	31
15	3.0 %-Au/MIL-101	IPA	20	343	Air	6
16	3.0 %-Au/MIL-101	KO^tBu	7	r.t.	Air	14
17	3.0 %-Au/MIL-101	KO^tBu	7	323	Air	74
18	3.0 %-Au/MIL-101	KO^tBu	7	363	Air	99

[a] Reaction conditions: 3.0 %-Au/MIL-101 (20 mg), benzyl alcohol (0.625 mmol), KO^tBu (0.20 mmol), toluene (5 mL), 343 K, Air.

aprotic toluene, which has high thermal conductivity and high oxygen solubility. Conversely, when polar protic IPA (isopropyl alcohol) with high thermal conductivity and good oxygen solubility was used as a solvent, the benzaldehyde yield was quite low. This may be due to the exchange of the labile Bronsted acidic protons with the solvent molecules and hence retarding the progress of the reaction [66] (Table 1, entries 13–15). Also, high selectivity to benzaldehyde of benzyl alcohol in toluene can be ascribed to the low solubility of water in this nonpolar solvent [6]. Because water is one of the products in this tandem prosess and the low solubility of water in the reaction medium could prevent the formation of over-oxidation products such as benzoic acid and benzyl benzoate. After that, we examined the influence of temperature on the this step (Table 1 entries 16–18). The yield of benzaldehyde was very low at room temperature (Table 1, entry 16). When we reduced the temperature from 343 K to 323 K, the yield of benzaldehyde was still low (Table 1, entry 17). In contrast, when we raised the temperature from 343 K to 363 K, there was no significant increase in the yield of benzaldehyde (Table 1, entry 18). Therefore, optimum temperature for high yield of benzaldehyde product was chosen as 343 K. Finally, the best result was observed when the benzyl alcohol oxidation reaction was carried out in toluene by using 20 mg of 3.0 %-Au/MIL-101 catalyst in the presence 0.625 mmol of benzyl alcohol and 0.20 mmol of KO^tBu at 343 K within 7 h.

After optimizing the reaction conditions for the oxidation step, we examined the reaction between benzyl alcohol and 4-chlorobenzylamine for the one-pot tandem synthesis (Step 1 + 2) of the corresponding imine (*i.e.* 0.625 mmol of benzyl alcohol, 0.625 mmol of 4-chlorobenzylamine, 0.20 mmol of KO^tBu, 20 mg of catalyst, 343 K, air atmosphere). The yield of related imine was 77 % after 8 h (Table 2, entry 1). This demonstrates the powerful multistep transformation activity of 3.0 %-Au/MIL-101. On the other hand, it is generally accepted that the condensation step proceeds in anerobic conditions. Therefore, although the presence of excess oxygen facilitates the oxidation step, it may be inhibiting the condensation step. Because, in the presence of excess oxygen, the amine in reaction can be oxidized. To control the effect of oxygen during the one-pot tandem reaction, we examined the reaction between benzyl alcohol and 4-chlorobenzylamine under different atmospheres; open flask/Ar, O_2 and air. When the reaction is carried out in an open flask under an Ar atmosphere, the the yield of related imine was 96 % after 8 h (Table 2, entry 2). In contrast, when the reaction is carried out under the O_2 atmosphere, the yield of imine was very low after 8 h and benzyl benzoate formation was observed as a by-

Table 2
Optimization of one-pot imine synthesis from alcohols and amines with 3.0 %Au/MIL-101[a].

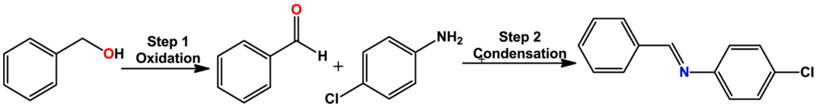

Entry	Reactions	Catalyst	Conditions	Time (h)	Yield of imine (%)	Selectivity of imine (%)
1	Steps 1 + 2	3.0 %-Au/MIL-101	Air	8	77	>99
2	Steps 1 + 2	3.0 %-Au/MIL-101	Open flask/Ar	8	96	>99
3	Steps 1 + 2	3.0 %-Au/MIL-101	O_2	8	10	55
4	Steps 1 + 2	None	Open flask/Ar	8	trace	>99
5	Steps 1 + 2	MIL-101	Open flask/Ar	8	4	>99
6	Step 2	MIL-101	Open flask/Ar	1	96	>99
7	Step 2	3.0 %-Au/MIL-101	Open flask/Ar	1	89	>99
8	Step 2	None	Open flask/Ar	1	64	>99

[a] Reaction conditions: 3.0 %-Au/MIL-101 (20 mg), amine (0.625 mmol), benzyl alcohol (0.625 mmol), KO^tBu (0.20 mmol), Toluene (5 mL), 343 K, Open flask/Ar.

product. (Table 2, entry 3). As a result, it can be said that amount of oxygen plays an important role in the one-pot tandem the synthesis of imine and so, all further experiments were performed in an open flask under an argon stream. Meanwhile, control experiments were performed under the optimized conditions to understand the function of Au/MIL-101 in the one-pot prosess. As expected, when using MIL-101 as the catalyst, only 4% of the corresponding imine was obtained because there were no Au NPs to promote the first oxidation step. Similarly, considerable imine formation was not observed without catalyst (Table 2, entries 4 and 5).

On the other hand, we separately investigated the condensation reaction between of the *in situ* generated benzaldehyde and 4-chlorobenzylamine (Step 2). When separately investigating the condensation reaction, MIL-101 with Lewis acidic sites showed excellent catalytic activity which is confirming the synergistic effects of acidic sites (Table 2, entry 6).In the presence of 3.0 %-Au/MIL-101, the activity slightly decreased, while in the absence of catalyst, yield of the corresponding imine was only 64 % (Table 2, entries 7 and 8). Thus, we suggest that MIL-101 promoted the condensation step. These results show that the active sites for both the oxidation and the condensation step were on the Au/MIL-101 catalyst.

By determining the optimized reaction conditions, the scope of this one-pot tandem reaction was examined by structurally and electronically diverse amines (Table 3). As is formerly disclosed the selective oxidation of benzyl alcohol is the key step in the one-pot tandem reaction. Thereby, the structure of chosen amines may likely have an effect on the conversion and product yield. The Au/MIL-101 catalyst shows a high imine yield (87–99 %) with the substituted anilines. On the other hand, located groups on the phenyl group of amines could change the nucleophilicity of aniline derivatives and thus promote the nucleophilic attack due to the nature and the position of substituents. As excepted, the reaction of benzyl alcohol with amines modified by electron-donating groups (*i.e.* $-CH_3$ and $-$ OCH_3) was faster than those with electron-withdrawing group (*i.e.* -Cl). Furthermore, it is found that the position of the substituent on the phenyl group of amines is also significant for the yield of related imine. For example, for *o*-, *m*- and *p*-Cl/OCH_3 substituents, the yields of related imines are in the order of para > meta > ortho substitution, indicating an influence of a steric effect. The conversion rate of 2,6-diisopropylaniline and 1-naphthylamine into the corresponding imines are lower than those of other substituted amines, but the selectivities are very good (Table 3). This decrease might be due to the limited diffusion of large-sized substrates in MIL-101. As a result, it can be said that Au/MIL-101 is a highly effective and selective catalyst for this one-pot reaction.

A important advantage of heterogeneous catalysis is the ability to smoothly remove the catalyst from the reaction and reuse it for next runs. In this regard, the reusing and recycling capability of 3.0 %-Au/MIL-101 were investigated for the one-pot imine synthesis, under optimum reaction conditions. After each catalytic run, the catalyst was collected by centrifugation and exhaustively washed with various solvents. After that, it was dried and used directly for the further runs under the same reaction conditions. After being used five cycles in successive reactions, the reaction conversion was still up to 97 % with 100 % selectivity (Fig. 6). Au/MIL-101 sample harvested from the fifth catalytic run was analyzed by TEM. The sum of its results showed that no obvious changes in the morphology of Au NPs (**Fig. S23**). The slight decrease (~3%) in the activity of Au/MIL-101 catalyst can be attributed to increase in the average size of Au NPs from 1.94 ± 0.16 nm to 2.12 ± 0.17 nm (Fig. S23). XRD analysis was also performed to determine the stability of the Au/MIL-101 catalyst. In **Fig. S24**, the XRD patterns of the fresh catalyst and the product obtained at the end of the 5th catalytic cycle are compared. It was observed that there was no significant change in the crystallinity of the Au/MIL-101 catalyst after reuse. A new diffraction peak observed at $2\theta = 27.46°$ in the product isolated after reuse experiment. It is estimated that this new diffraction peak may arise from the base (KO^tBu) used in the catalytic study. These results indicate

Table 3
3.0 %-Au/MIL-101- catalysed one-pot imine formation from benzyl alcohol and various amines.

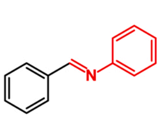 8h 99% (>99%), TOF = 51.47 h^{-1}	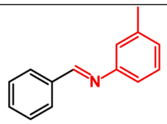 8h 96% (>99%), TOF = 49.91 h^{-1}	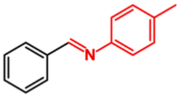 8h 99% (>99%), TOF = 51.47 h^{-1}
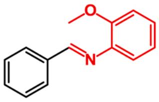 8h 93% (>99%), TOF = 48.35 h^{-1}	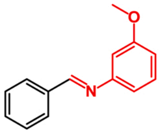 8h 96% (>99%), TOF = 49.91 h^{-1}	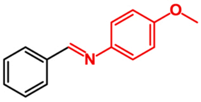 8h 99% (>99%), TOF = 51.47 h^{-1}
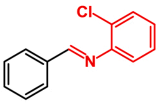 8h 89% (>99%), TOF = 46.27 h^{-1}	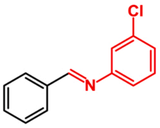 8h 92% (>99%), TOF = 47.83 h^{-1}	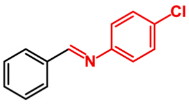 8h 96% (>99%), TOF = 49.91 h^{-1}
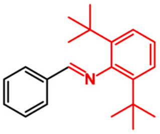 12h 97% (>99%), TOF = 33.62 h^{-1}	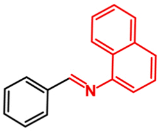 12h 87% (>99%), TOF = 30.15 h^{-1}	

---

[a] Reaction conditions: 3.0 %-Au/MIL-101 (20 mg), amine (0.625 mmol), benzyl alcohol (0.625 mmol), KO^tBu (0.20 mmol), Toluene (5 mL), 343 K, Open flask/Ar. The selectivity of corresponding imine is given in parentheses.

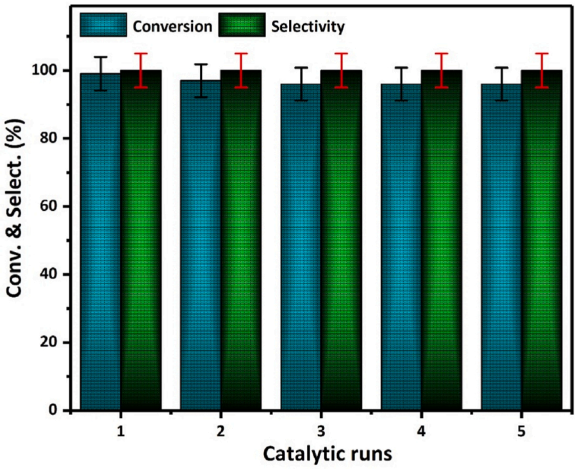

Fig. 6. The reusability of Au/MIL-101 catalyst along the one-pot imine synthesis.

that Au/MIL-101 catalyst was stable under the current one-pot imine formation from benzyl alcohol and amines conditions and could be reused for multiple runs of the cross coupling of alcohols and amines. The heterogeneous catalytic nature of Au/MIL-101 was confirmed by the hot leaching test for both the oxidation and condensation steps. In both reactions, the conversion in the presence Au/MIL-101 as a catalyst gradually increased from 0 to 3 h. To demonstrate that no Au NPs were dissolved in the solvent during the reactions, the Au/MIL-101 catalyst was removed after 3 h and reaction was carried out under the same conditions for an additional 5 h (**Figs. S25-26**). The reaction no longer proceeded when the catalyst was removed. Consequently, during the reactions, there were no Au NPs leaching into the reaction medium, and MIL-101 as a carrier perfectly keeped the loading Au NPs.

Until now, a number of catalyst systems have been employed to synthesize imine derivatives *via* oxidative coupling of amines and alcohols. However, most of them suffer from harsh reaction conditions (high gase pressure and high temperature), long reaction time, limited substrate scope and low turnover number/frequency (TON and TOF). A comparison between the catalytic activities of prepared catalyst and other reported catalysts systems in the synthesis of *N*-benzylideneaniline from aniline and benzyl alcohol was made, and the results are given in Table 4 [56,60,67–78]. Long et al. have developed a base-free catalytic system using CeO_2 immobilized on magnetic core-shell microparticles as catalyst. The alkalinity of the prepared catalysts enabled this tandem reaction to run in a without base environment, but it suffers from low turnover frequency (TOF =3.96 h^{-1}) [79] (Table 4, entry 1). Tan and co-workers reported $Ni_3(OH)(COO)_6$−based MOF catalyst system, through which imines can be obtained in the presence of KOH under solvent free conditions although it requires high temperature (373 K) to promote the reaction and long reaction time (12 h, the selectivity of imine 88 %) [80] (Table 4, entry 2). Chen et. al. and Mandal et. al. have reported active 5.0 wt% MnO_x/HAP [81] and MnO_x/TiO_2@SBA-15 [75] as catalysts, respectively, any base was not required for imine synthesis and reactions carried out ambient conditions (Table 4, entries 3–4). But high imine yields were achieved only with a high amount of catalyst and long reaction time (24 h). Although the active catalytic species of MnOx/HAP have not yet been fully clarified by Chen et al., both HAP and MnOx/HAP were found to obviously promote the condensation step, which can be attributed to the utility of Lewis acid sites of the catalyst. On the other hand, in the reaction pathway proposed by Mandal et al., the role of MnO_2 is to produce O_2- species without oxygen splitting by adsorbing oxygen to the Mn^{3+} region. This O_2- species adsorbed on Ti^{4+} gives rise to Ti-O-O- species. This Ti-O-O- species acts as an active oxidizing species and benzyl alcohol gets oxidized in presence of Ti-O-O- species and produce benzaldehyde. The interaction of aniline on weak acid site (Si−OH) of SiO_2 lead to formation of imine [81].

Moreover, there are many other heterogeneous catalysts such as Au/HAP [49], Au/TiO_2 [67,77,78], Au/$ZnAl_2O_3$ [56], Au-Pd/ZrO_2 [69],

Table 4
One-pot synthesis of *N*-benzylidenaniline from benzyl alcohol and aniline with reported various heterogeneous catalyst.

Entry	Catalyst	Base	Conditions	Temp. (°C)	Time (h)	Yield of imine (%)	TOF (h^{-1})	Ref.
1[a]	Fe_3O_4@X@CeO_2	–	Air	60	12	–	3.96	[76]
2	$Ni_3(OH)(COO)_6$−based MOF	KOH	Air ballon	100	12	88	–	[80]
3	MnOx/HAP	–	Air ballon	80	24	93	–	[81]
4[b]	MnOx/TiO_2@SBA-15	–	Air	80	24	93	–	[75]
5	TiO_2@PMHSIPN	K_2CO_3	Ar	160	12	94	–	[83]
6[c]	Ag/Al_2O_3	Cs_2CO_3	Air	125	25	100	–	[73]
7[d]	CdS@MIL-101	–	Air, $\lambda > 420$ nm	0	10	53	–	[74]
8	Au/$ZnAl_2O_3$	–	Air	60	8	99	39.1	[56]
9	Au/HAP	–	O_2 bubbling	60	3	99		[60]
10[e]	Au/TiO_2	CH_3OK	O_2	20	24	7	–	[67]
11	Au/TiO_2	–	O_2 bubbling	60	36	88	–	[77]
12[f]	Au/TiO_2	–	0.5 MPa O_2	120	22	45	–	[18]
13[g]	Au/TiO_2	Cs_2CO_3	0.1 MPa N_2	110	22	22	–	[18]
14[h]	Au/TiO_2	Cs_2CO_3	5 atm N_2	120	14	≈ 50	–	[78]
15[i]	Au/TiO_2	–	5 atm N_2	120	14	7.5	–	[78]
16[j]	PICB-Au/Pd	NaOH	O_2	30	12	70	–	[68]
17[k]	Au–Pd@ZrO_2	–	Air	40	8	94	79[c]	[69]
18[l]	PdAu@MIL-100(Fe)	–	N_2, light irradiation	R.T.	24	5	–	[70]
19	Pd − Au@Mn(II)-MOF	KOH	Air	110	30	99	4.4	[71]
20[m]	Cu-MOF nanorod/Au–Pd	–	Air	110	18	91	–	[72]
21	**Au/MIL-101**	**KO^{t}Bu**	**Open flask/Ar**	**70**	**8**	**99**	**51.47**	**This study**

[a] Amine (2.0 mmol), alcohol (1.0 mmol), Fe_3O_4@CN@CeO_2 (20 mg); [b] Amine (1.0 mmol), Alcohol (1.0 mmol), catalyst (100 mg); [c] Amine (1.5 mmol), Alcohol (3 mmol), 2.4 wt.%Ag/Al_2O_3 (165 mg), Cs_2CO_3 (100 mg); [d] Amine 0.1 mmol, Alcohol (0.15 mmol), CdS(2 wt.%)@MIL-101 100 mg; [e] Alcohol (20 mmol), Amine (20 mmol), base (2 mmol) and methanol (50 mmol) and Au/substrate molar ratio of 1/4500; [f] Azobenzene was formed as a by-product, [g] Amine, ester, amide were as by-products; [h] N-phenylbenzylamine (*ca.*50 %) was formed as a by-product, [i] Main product was N-phenylbenzylamine (*ca.* 93 %); [j] Amine (0.368 mmol), Alcohol (0.368 mmol), NaOH (0.095 mmol), PICB-Au/Pd (0.0057 mmol, 1.5 mol%), THF/CF_3CH_2OH (9:1, 0.5 mL); [k] The reaction was carried out in a one-pot, two-step method. In the first step, benzyl alcohol was oxidized to benzaldehyde. The second step reaction commenced by adding stoichiometric amount of aniline after the first step reaction was completed. TOF is measured at t =1 h, [l] Amine (0.1 mmol), Alcohol (3 mmol), CH_3CN (2 mL), catalyst (10 mg); [m] Alcohol (1.04 mmol), aniline (1.24 mmol) and catalyst (4 mg).

Ir-Zr-MOF [82], *etc.* The Au/$ZnAl_2O_3$ catalyst presented the high performance among the reported Au catalysts at mild temperatures with high TOF =39.1 h^{-1}, due to the active surface oxygen species and the acidic-basic property of support, but it suffer from limited substrate scope (Table 4, entry 8) [56]. Similarly, Au/HAP as catalyst displayed high performance at 60 °C and after 3 h the yield and selectivity of imine was 99 %, but in this reaction substrat/catalyst molar ratio was 100. In this base-free system, a delicate cooperation between metallic gold and the acid/base sites of the hydroxyapatite (HAP) surface was play a key role in determining the efficiency and compatibility of the Au/HAP catalyst for not only the rate-determining alcohol oxidation but also for the subsequent condensation step of the tandem reaction (Table 4, entry 9) [60].

On the other hand, the catalytic activity of Au/TiO_2 in oxidative coupling of amines and alcohols has been studied by several groups in the absence and/or presence base (Table 4, entries 11–15) [67,77,78]. According to these studies, product selectivity (imine, amine and others) depends on significantly to reaction conditions such as temperature, base and oxygen (Table 4, entries 4–7). In the examples reported by Sun et al. and Ishida e. al., when the reactions carried out without base at 60 and 120 °C under O_2 atmosphere, the yield of imine was 88 (after 36 h) and 45 % (after 22 h), respectively. Azobenzene was formed as by-product due to the direct aerobic oxidation of aniline in the presence of excess oxygen (Table 4, entries 4 and 7). Ishida et al. also reported that when the reactions performed with a base under 0.1 MPa N_2 pressure, the imine selectivity was low (secondary amine, ester, amide were formed as by-products). The results of He et al. were interesting for this tandem reaction. According to the report, in a base-free system under 5 atm N_2 at 120 °C, the main product was secondary amine, while imine was formed only as a byproduct. The adding of base to the reaction lead to formation of the imine product (after 14 h, *ca.* 50 %) [78].

There is a very limited number of MOF-based catalysts for the one-pot imine synthesis from alcohols and amines (Table 2, entries 18–20). Among all the ever-reported MOF-based catalysts, the prepared 3.0 %-Au/MIL-101 catalyst exhibited the highest TOF (51.47 h^{-1}) for one-pot synthesis of *N*-benzylidenaniline from benzyl alcohol and aniline.

3.3. Mechanism study of the reactions

The above experimental findings suggest that the catalytic pathway for efficient one-pot imine formation using Au/MIL-101 can be explained in Fig. 7. First, alcohol forms an alcoholate with the assistance of the base, and it binds to unsaturated Au atoms bearing positive charge density located at corners, edges and steps of the NPs. Then, Au-H and Au-alkoxide species form with the transfer of a α-H ($-CH_2$-) from the alcoholate to Au atoms. This is generally regarded as the initial step along alcohol oxidation over Au surfaces [2,34]. The role of oxygen in the reaction medium in this stage is to remove the hydrogen from corners/edges/steps of the Au NPs, leading to the catalytic cycle. After that, by removing a hydrogen from the Au-alkoxide, the desired benzaldehyde product is produced (Step 1).

After the benzaldehyde formed, the reaction can proceed in two possible pathways: *(i)* the produced benzaldehyde with a water molecule to form gem-diol, which can be oxidized into carboxylic acid intermediate or *(ii)* the produced benzaldehyde with amine molecule to form instable carbinolamine intermediate. We predicted that the reaction pathway proceeds through an unstable carbinolamine intermediate because carboxylic acid was not observed during the reaction in our system. MIL-101 has a high density of open chromium centres, which can act as Lewis acid sites for catalysis and along possible pathway, the C═O group of the benzaldehyde coordinates with this Lewis acid sites, which increases the electrophilicity of the C═O group [84]. Probably this nucleophilic attack effectively prevents the formation of over-oxidized by-products. Then, as a result of the nucleophilic addition reaction to the C═O group of the unreacted amine, an carbinolamine is formed. The formed unstable carbinolamine undergoes dehyration by acid-catalyzed a pathway to form the corresponding imine (Step 2). Consequently, Au/MIL-101 catalyst is appropriate material for the one pot tandem synthesis of imines because Au NPs offer oxidation activity while MIL-101 provides Lewis acid sites during the condensation step.

4. Conclusions

In conclusion, an efficient and stable bifunctional Au/MIL-101 catalyst was successfully developed by using the liquid phase impregnation method which showed excellent catalytic performance when applied in the one-pot tandem synthesis of various imines. The effects of various factors on the catalytic activity such as reaction atmosphere, solvent, temperature and base have been also investigated. We found that amount of oxygen and base are necessary for the high selectivity to benzaldehyde of benzyl alcohol which is the rate-determining step for

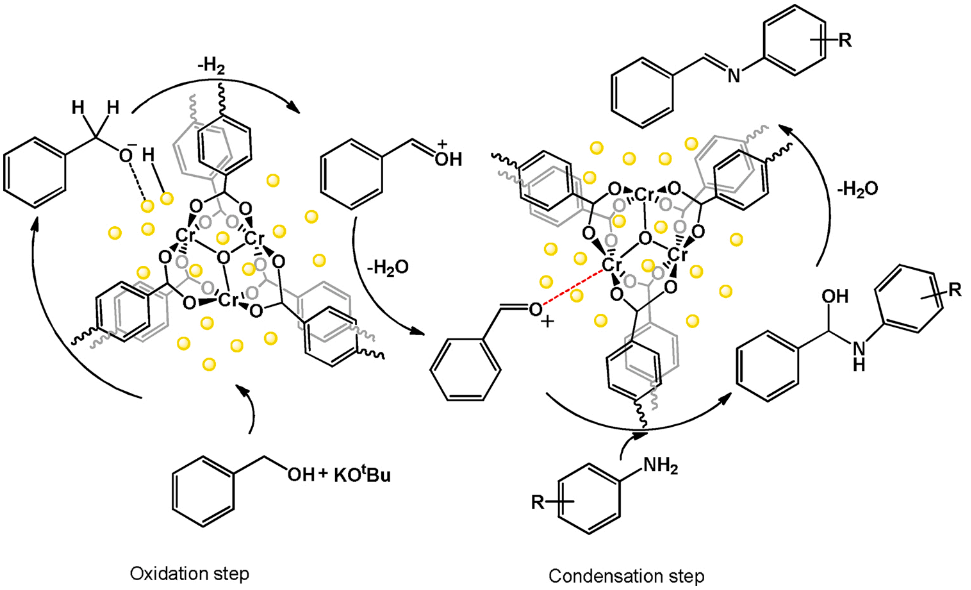

Fig. 7. Possible reaction pathway for the one-pot imine synthesis (yellow colored balls represent Au atoms) (For interpretation of the references to colour in this figure legend, the reader is referred to the web version of this article).

this one-pot reaction. A plausible catalytic reaction mechanism was proposed and it was found that Au NPs were highly effective in activating selective oxidation of benzyl alcohol to benzaldehyde, while the Lewis acid sites of MIL-101 catalyze the second condensation step without interfering with the oxidation step. Furthermore, prepared bifunctional catalyst was recyclable and could be reused for at least five times, demonstrating its excellent capacity in industrial catalysis. To our knowledge, bifunctional Au/MIL-101 catalyst has the highest TOF values among all the ever-reported MOF-supported catalysts.

CRediT authorship contribution statement

Ilkay Gumus: Conceptualization, Data curation, Formal analysis, Writing - review & editing. **Adem Ruzgar:** Investigation, Methodology, Software, Visualization, Writing - original draft. **Yasar Karatas:** Investigation, Methodology, Software, Visualization, Writing - original draft. **Mehmet Gülcan:** Conceptualization, Formal analysis, Supervision, Writing - review & editing.

Declaration of Competing Interest

The authors declare that they have no known competing financial interests or personal relationships that could have appeared to influence the work reported in this paper.

Acknowledgement

We would like to thank Van Yüzüncü Yıl University Research Fund for their contributions.

Appendix A. Supplementary data

Supplementary material related to this article can be found, in the online version, at doi:https://doi.org/10.1016/j.mcat.2020.111363.

References

[1] Y.B. Huang, J. Liang, X.S. Wang, R. Cao, Chem. Soc. Rev. 46 (2017) 126–157.
[2] A. Dhakshinamoorthy, A.M. Asiri, H. Garcia, ACS Catal. 7 (2017) 2896–2919.
[3] A. Dhakshinamoorthy, H. Garcia, ChemSusChem 7 (2014) 2392–2410.
[4] F.X. Felpin, E. Fouquet, ChemSusChem 1 (2008) 718–724.
[5] Y. Hu, J. Zhang, H. Huo, Z. Wang, X. Xu, Y. Yang, K. Lin, R. Fan, Catal. Sci. Technol. 10 (2020) 315–322.
[6] Y. Liu, X.-C. Ma, G.-G. Chang, S.-C. Ke, T. Xia, Z.-Y. Hu, X.-Y. Yang, J. Colloid Interface Sci. 557 (2019) 207–215.
[7] X. Chen, S. Han, D. Yin, C. Liang, Inorg. Chem. Front. 7 (2020) 82–90.
[8] Y. Zhang, Y. Wang, L. Liu, N. Wei, M.-L. Gao, D. Zhao, Z.-B. Han, Inorg. Chem. 57 (2018) 2193–2198.
[9] S. Ke, G. Chang, Z. Hu, G. Tian, D. Yang, X. Ma, K. Huang, J. Li, X. Yang, ACS Sustainable Chem. Eng. 8 (2020) 966–976.
[10] A. Das, N. Anbu, M. SK, A. Dhakshinamoorthy, S. Biswas, Eur. J. Inorg. Chem. 29 (2020) 2830–2834.
[11] F.G. Cirujano, A. Leyva-Pérez, A. Corma, F.X. Llabrés i Xamena, ChemCatChem. 5 (2013) 538–549.
[12] A. Dhakshinamoorthy, A.M. Asiri, H. García, Trends Analyt. Chem. 2 (5) (2020) 454–466.
[13] A. Dhakshinamoorthy, A.M. Asiri, H. Garcia, Chem. Commun. (Camb.) 53 (2017) 10851–10869.
[14] L.Y. Chen, Q. Xu, Matter 1 (2019) 57–89.
[15] S. Xing, J. Li, G. Niu, Q. Han, J. Zhang, H. Liu, Mol. Catal. 458 (2018) 83–88.
[16] W. Li, Z. Cai, H. Li, Y. Shen, Y. Zhu, H. Li, X. Zhang, F. Wang, Mol. Catal. 472 (2019) 17–26.
[17] F. Ke, J. Zhu, L.-G. Qiu, X. Jiang, Chem. Commun. (Camb.) 49 (2013) 1267–1269.
[18] T. Ishida, N. Kawakita, T. Akita, M. Haruta, Gold Bull. 42 (2009) 267–274.
[19] X. Li, T.W. Goh, L. Li, C. Xiao, Z. Guo, X.C. Zeng, W. Huang, ACS Catal. 6 (2016) 3461–3468.
[20] A. Corma, H. García, F.X. Llabrés i Xamena, Chem. Rev. 110 (2010) 4606–4655.
[21] Z. Wang, S.M. Cohen, Chem. Soc. Rev. 38 (2009) 1315–1329.
[22] Z. Zhang, L. Zhang, L. Wojtas, P. Nugent, M. Eddaoudi, M.J. Zaworotko, J. Am. Chem. Soc. 134 (2012) 924–927.
[23] K. Vellingiri, L. Philip, K.-H. Kim, Coord. Chem. Rev. 353 (2017) 159–179.
[24] B. Li, K. Leng, Y. Zhang, J.J. Dynes, J. Wang, Y. Hu, D. Ma, Z. Shi, L. Zhu, D. Zhang, Y. Sun, M. Chrzanowski, S. Ma, J. Am. Chem. Soc. 137 (2015) 4243–4248.
[25] A. Dhakshinamoorthy, A.M. Asiri, H. García, Trends Analyt. Chem. 2 (5) (2020) 454–466.
[26] S. Rostamnia, F. Mohsenzad, Mol. Catal. 445 (2018) 12–20.
[27] W.-J. Sun, E.-Q. Gao, Mol. Catal. 482 (2020), 110746.
[28] H. Liu, G. Chen, H. Jiang, Y. Li, R. Luque, ChemSusChem 5 (2012) 1892–1896.
[29] J.-S. Wang, F.-Z. Jin, H.-C. Ma, X.-B. Li, M.-Y. Liu, J.-L. Kan, G.-J. Chen, Y.-B. Dong, Inorg. Chem. 55 (2016) 6685–6691.
[30] P. Huang, W. Ma, P. Yu, L. Mao, Chem. - Asian J. 11 (2016) 2705–2709.
[31] Y.-Y. Zhang, J.-X. Li, L.-L. Ding, L. Liu, S.-M. Wang, Z.-B. Han, Inorg. Chem. 57 (2018) 13586–13593.
[32] Y.Z. Chen, Y.X. Zhou, H. Wang, J. Lu, T. Uchida, Q. Xu, S.H. Yu, H.L. Jiang, ACS Catal. 5 (2015) 2062–2069.
[33] Z. Li, R. Yu, J. Huang, Y. Shi, D. Zhang, X. Zhong, D. Wang, Y. Wu, Y. Li, Nat. Commun. 6 (2015) 8248.
[34] Y. Qi, Y. Luan, X. Peng, M. Yang, J. Hou, G. Wang, Eur. J. Inorg. Chem. 30 (2015) 5099–5105.
[35] J.P. Adams, J. Chem. Soc. Perkin Trans. I 1 (2000) 125–139.
[36] H. Sharma, N. Singh, D.O. Jang, Green Chem. 16 (2014) 4922–4930.
[37] D. Wang, Z. Li, J. Catal. 342 (2016) 151–157.
[38] Y. Shiraishi, M. Ikeda, D. Tsukamoto, S. Tanaka, T. Hirai, Chem. Commun. (Camb.) 47 (2011) 4811–4813.
[39] J.F. Soulé, H. Miyamura, S. Kobayashi, J. Am. Chem. Soc. 133 (2011) 18550–18553.
[40] A. Abad, P. Concepcon, A. Corma, H. Garcia, Angew. Chem. Int. Ed. 44 (2005) 4066–4069.
[41] B. Gole, U. Sanyala, P.S. Mukherjee, Chem. Commun. (Camb.) 51 (2015) 4872–4875.
[42] H. Miyamura, R. Matsubara, Y. Miyazaki, S. Kobayashi, Angew. Chem. Int. Ed. 46 (2007) 4151–4154.
[43] L. Bromberg, Y. Diao, H. Wu, S.A. Speakman, T.A. Hatton, Chem. Mater. 24 (2012) 1664–1675.
[44] I.E. Ertas, M. Gulcan, A. Bulut, M. Yurderi, M. Zahmakiran, J. Mol. Catal. A Chem. 410 (2015) 209–220.
[45] I.E. Ertas, M. Gulcan, A. Bulut, M. Yurderi, M. Zahmakiran, Microporous Mesoporous Mater. 226 (2016) 94–103.
[46] N. Konuş, Y. Karataş, M. Gülcan, Synth. React. Inorg. M. 46 (2016) 534–542.
[47] M. Kanat, Y. Karataş, M. Gülcan, B. Anıl, Int. J. Hydrogen Energ. 43 (2018) 22548–22556.
[48] G.H. Woehrle, J.E. Hutchıson, S. Ozkar, R.G. Finke, Turk. J. Chem. 30 (2006) 1–13.
[49] T. Nakamura, Y. Mochidzuki, S. Sato, J. Mater. Res. 23 (2008) 968–974.
[50] R.T. Mendieta, D.V. Espinosa, S. Sabater, J. Lancis, G. Mínguez-Vega, J.A. Mata, Sci. Rep. 6 (2016) 30478.
[51] J.P. Sylvestre, S. Poulin, A.V. Kabashin, E. Sacher, M. Meunier, J.H.T. Luong, J. Phys. Chem. B 108 (2004) 16864–16869.
[52] D.K. Božanić, A.S. Luyt, L.V. Trandafilovića, V. Djoković, RSC Adv. 3 (2013) 8705–8713.
[53] J. Li, B. Tian, T. Li, S. Dai, Y. Weng, J. Lu, X. Xu, Y. Jin, R. Pang, Y. Hua, Int. J. Nanomedicine 13 (2018) 1411–1424.
[54] Z. Wang, Q. Zhang, D. Kuehner, A. Ivaskab, L. Niu, Green Chem. 10 (2008) 907–909.
[55] L. Cheng, X. Li, J. Dong, J. Mater. Chem. C Mater. Opt. Electron. Devices 3 (2015) 6334–6340.
[56] S. Wu, W. Sun, J. Chen, J. Zhao, Q. Cao, W. Fang, Q. Zhao, J. Catal. 377 (2019) 110–121.
[57] J. Qin, Y. Long, W. Wu, W. Zhang, Z. Gao, J. Ma, J. Catal. 371 (2019) 161–174.
[58] M. Zhang, S. Wu, L. Bian, Q. Cao, W. Fang, Catal. Sci. Technol. 9 (2019) 286–301.
[59] R.A. Sheldon, H. van Bekkum, Fine Chemicals Through Heterogeneous Catalysis, John Wiley & Sons Inc., Hoboken, NJ, 2001 pp 1–636.
[60] H. Sun, F.Z. Su, J. Ni, Y. Cao, H.Y. He, K.N. Fan, Angew. Chem. Int. Ed. 48 (2009) 4390–4393.
[61] I. Gumus, Y. Karatas, M. Gülcan, Catal. Sci. Technol. 10 (2020) 4990–4999.
[62] S. Storck, H. Bretinger, W.F. Maier, Appl. Catal. A Gen. 134 (1998) 137.
[63] R.S.H. Mikhail, S. Brunauer, E.J. Bodor, J. Colloid Interface Sci. 26 (1968) 45.
[64] C.P. Ferraz, M.A.S. Garcia, E. Teixeira-Neto, L.M. Rossi, RSC Adv. 6 (2016) 25279–25285.
[65] S. Sadiq, M. Sadiq, K. Saeed, N.U. Rehman, Q. Ali, React. Kinet. Mech. Catal. 130 (2020) 289–302.
[66] A.C. Sunil Sekhar, A.E. Ashokkumar, C.T. Cygnet, S. Vidhya Lakshmi, F.L. Deepak, C.P. Vinod, ChemNanoMat 4 (2018) 537–541.
[67] S. Kegnæs, J. Mielby, U.V. Mentzel, C.H. Christensen, A. Riisager, Green Chem. 12 (2010) 1437–1441.
[68] J.F. Soulé, H. Miyamura, S. Kobayashi, Chem. Commun. (Camb.) 49 (2013) 355–357.
[69] W. Cui, Q. Xiao, S. Sarina, W. Ao, M. Xie, H. Zhu, Z. Bao, Catal. Today 235 (2014) 152–159.
[70] D. Wang, Y. Pan, L. Xu, Z. Li, J. Catal. 361 (2018) 248–254.
[71] G.J. Chen, H.C. Ma, W.L. Xin, X.B. Li, F.Z. Jin, J.S. Wang, M.Y. Liu, Y.B. Dong, Inorg. Chem. 56 (2017) 654–660.
[72] M. Zhong, S. Zhang, A. Dong, Z. Sui, L. Feng, Q. Chen, J. Mater. Sci. 55 (2020) 10388–10398.
[73] H. Liu, G.-K. Chuah, S. Jaenicke, J. Catal. 292 (2012) 130–137.
[74] R. Wu, S. Wang, Y. Zhou, J. Long, F. Dong, W. Zhang, ACS Appl. Nano Mater. 2 (2019) 6818–6827.
[75] S. Mandal, S. Maity, S. Saha, B. Banerjee, RSC Adv. 6 (2016) 73906–73914.
[76] Y. Long, Z. Gao, J. Qin, P. Wang, W. Wu, L. Zhang, Z. Dong, J. Ma, J. Colloid Interface Sci. 538 (2019) 709–719.
[77] H. Sun, F.-Z. Su, J. Ni, Y. Cao, H.-Y. He, K.-N. Fan, Angew. Chem. Int. Ed. 48 (48) (2009) 4390–4393.

[78] L. He, X.-B. Lou, J. Ni, Y.-M. Liu, Y. Cao, H.-Y. He, K.-N. Fan, Chem. Eur. J. 19 (2010) 13965–13969.
[79] Y. Long, Z. Gao, J. Qin, P. Wang, W. Wu, L. Zhang, Z. Dong, J. Ma, J. Colloid Interface Sci. 538 (2019) 709–719.
[80] J.-Y. Tan, J.-X. Shi, P.-H. Cui, Y.-Y. Zhang, N. Zhang, J.-Y. Zhang, W. Deng, Microporous Mesoporous Mater. 287 (2019) 152–158.
[81] B. Chen, J. Li, W. Dai, L. Wang, S. Gao, Green Chem. 6 (2014) 3328–3334.
[82] A.M. Rasero-Almansa, A. Corma, M. Iglesias, F. Sanchez, ChemCatChem 6 (2014) 1794–1800.
[83] H. Wang, J. Zhang, Y.-M. Cui, K.-F. Yang, Z.-J. Zheng, L.-W. Xu, RSC Adv. 4 (2014) 34681–34686.
[84] E. Niknam, F. Panahi, F. Daneshgar, F. Bahrami, A. Khalafi-Nezhad, ACS Omega 3 (2018) 17135–17144.